JOURNAL OF MATERIALS SCIENCE 16 (1981) 1071–1080

Thermochemical dissolution of corundum

A. E. SMIRNOV, A. A. URUSOVSKAYA, V. G. GOVORKOV, G. V. BEREZHKOVA
Institute of Crystallography, USSR Academy of Sciences, V-333 Moscow, USSR

The ideal dissolution forms of crystals are discussed. The ideal dissolution form of corundum is compared with its real forms, obtained under different experimental conditions, and with its simple forms expected on the basis of structural observations. Anisotropy of the dissolution rates of sapphire and ruby spheres is shown. On the basis of kinetic data it is concluded that the rate of the chemical reaction between corundum and reagent controls the thermochemical dissolution of corundum. The possible chemical reactions determining dissolution are estimated.

1. Introduction

The chemical treatment of chemically stable refractory crystals is rather difficult. Corundum is such a crystal. Methods for the chemical treatment of corundum can be divided into dissolution in liquids, in melts and in the gas phase.

High-temperature dissolution in acid and alkaline solutions was used for investigating the dislocation structure of corundum. A borax melt was used for chemical polishing [1–4]. Dissolution of monocrystal spheres of sapphire was carried out with the aim of obtaining dissolution forms and investigating their morphology. Dissolution was carried out in 0.1 M solutions of K_2HPO_4, KH_2PO_4, K_2SiO_3, K_2CO_3, KF and NaF under hydrothermal conditions at 600° C and 3 kbar; and also in melts of $K_2S_2O_7$, $PbO:PbF_2$ [5]. For etching and polishing α-Al_2O_3 a number of gas organic etchants were used i.e. CHF_3, $CHFCl_2$, CF_4, CF_6 and others [6], as well as H_2 [7].

An effective corundum gas-etching method is thermochemical dissolution in CO [8, 9]. This method consists of the dissolution of corundum at a high temperature resulting in chemical reaction between corundum and CO (or C) with the formation of volatile reaction products.

An analysis of the literature on the dissolution of corundum in solutions, melts and the gas phase shows that investigators have been concentrating their attention mainly on the morphology of dissolution forms. These forms are a function of the physico-chemical conditions of the experiment. The monocrystal sphere is the most convenient form for studying the morphology of the dissolution surface, hence the principal studies were carried out on spheres. However, it is difficult to compare these results because some authors indicated the dissolution forms by the vertices [10–12], while others indicated the faces [5]. Data on dissolution kinetics are scarce [7, 13]. This paper presents some results of research into the dissolution forms of sapphire and ruby monocrystal spheres.

2. Experimental procedure

Monocrystals of sapphire and ruby grown from a melt at the Institute of Crystallography, USSR Academy of Sciences were used. The impurity content was Cr–3×10^{-3} wt%, Mu–1.8×10^{-4} wt%, Mg–1.5×10^{-3} wt%, V–5×10^{-4} wt%, Ga–1×10^{-3} wt%, Mo–1.8×10^{-4} wt% and Cu–5×10^{-5} wt%. The Cr content of ruby was 7.5×10^{-2} wt%.

The spheres of sapphire and ruby (~ 15 mm in diameter) were placed in graphite containers according to our previous method [11]. Both the container with the sapphire sphere and the container with the ruby sphere were placed in a reaction chamber. Thus the conditions of dissolution of the sapphire and ruby spheres were identical. The spheres were dissolved in the temperature range 1400 to 1700° C. Earlier experiments with dissolution–time variation showed the optimal time to be 6 h [11]. During this time

0022–2461/81/041071–10$03.00/0

all vertices and edges appeared on the surface of the sphere according to the dissolution form of corundum under the given experimental conditions.

The ZR J–3 optical goniometer was used for the determination of the vertex-indices on the dissolution forms. Distances between opposite vertices were measured using a micrometer with conic nozzles. The dissolution rate was taken as the quantitative parameter of the investigation. This value was determined from the ratio of the distance between opposite vertices to the dissolution time.

The reaction products of corundum with C and CO were identified on an AVF-202E X-ray diffractometer.

3. Results

3.1. Morphology of dissolution form

As a result of dissolution at 1400 to 1700° C the initial sapphire and ruby spheres acquired definite forms [the real form of dissolution which is a polyhedron with 26 vertices corresponding to: 0001: (or :001: in *hkl* designations), rhombohedron :02$\bar{2}$1: (:021:), prism :11$\bar{2}$0: (:110:) and dipyramid :11$\bar{2}$3: (:113:)]. The number and arrangement of the vertices and edges on the sapphire and ruby dissolution forms are the same (Fig. 1). The faces left after dissolution exhibit some etching. The ruby sphere has a rougher surface micro-relief compared to sapphire.

3.2. Kinetic data

Measurement of the dissolution rates along the crystallographic directions corresponding to the vertices on the sphere, revealed definite anisotropy. The lowest dissolution rate was observed along the ⟨001⟩ direction, for both sapphire and ruby spheres. The dissolution rate of ruby is higher compared to sapphire at the same temperature and along the same crystallographic direction (Table 1).

Based on the data obtained, the polar diagrams of the dissolution rates on the (001) face were drawn (Table I).

The data on the dissolution rates in the 1400 to 1700° C temperature range permitted calculation of the ratio $lgV : 1/T$ for sapphire and ruby along the four crystallographic directions (Fig. 2a and b), where V is the volume and T is the temperature. In the case of sapphire this ratio takes the form of straight lines for the directions ⟨001⟩, ⟨110⟩ and ⟨021⟩. At 1500° C [or $56 \times 10^5/T$ (K^{-1})] the line breaks in the direction ⟨113⟩ (Fig. 2a). For dissolution of the ruby spheres all the lgV–$1/T$ lines have a break at the same temperature in the four directions (Fig. 2b).

The activation energy calculated by means of the known formula: $E = (k\Delta lu V)/(\Delta 1/T)$, was found to be $E_1 = 3.95$ eV, $E_2' = 4.45$ eV and $E_2'' = 0.99$ eV (Fig. 2a) for sapphire and $E_3 = 7.41$ eV and $E_4 = 1.48$ eV (Fig. 2b) for ruby. The designations are clear from Fig. 2a and b.

X-ray analysis of the reaction products precipitated on the walls of the container showed that Al_4C_3 is a reaction product.

4. Discussion

4.1. Ideal dissolution forms of crystals

First the morphology of the growth and dissolution forms of crystals will be discussed. According to the hypothesis of Wulff [14], crystal faces grow at a rate inversely related to their reticular density. Given such growth, the greater the distance of each face from the centre of growth, the longer

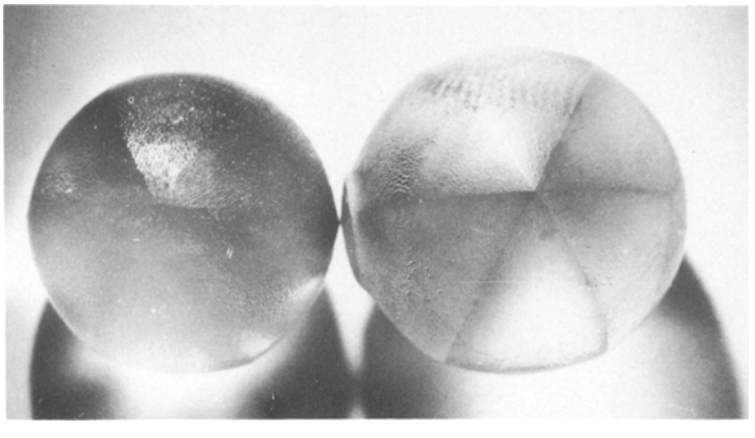

Figure 1 Real dissolution forms of spheres of ruby (left) and sapphire (right) obtained by thermochemical dissolution methods.

TABLE I

T (° C)	$h\,k\,l$	Dissolution rate (mm h^{-1})		Polar diagrams	
		Sapphire	Ruby	Sapphire	Ruby
1500	0 0 1	0.033	0.396	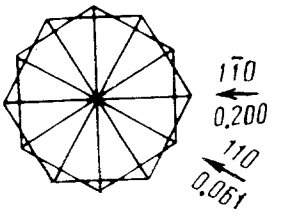	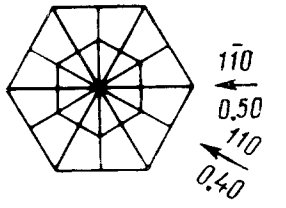
	1 1 0	0.061	0.445		
	0 2 1	0.085	0.530		
	1 1 3	0.100	0.538		
1600	0 0 1	0.085	0.475	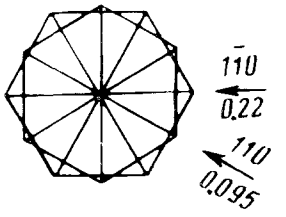	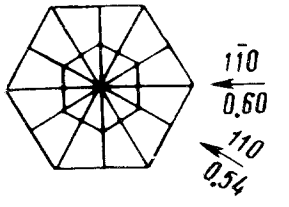
	1 1 0	0.095	0.535		
	0 2 1	0.110	0.685		
	1 1 3	0.210	0.695		
1700	0 0 1	0.330	0.860	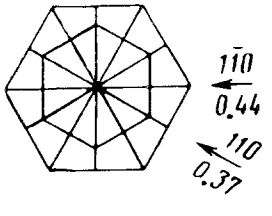	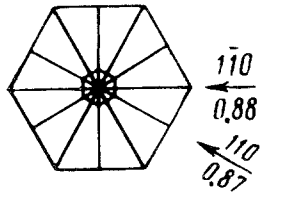
	1 1 0	0.370	0.870		
	0 2 1	0.380	0.900		
	1 1 3	0.400	0.960		

the corresponding reciprocal lattice vector perpendicular to it must be. The faces nearest to the centre of growth will form into a convex polyhedron. Delaunay *et al.* [15] proved that there are 24 different kinds of such polyhedra in all lattices. Delaunay called these polyhedra "Wulff's ideal habits". These polyhedra (ideal growth forms) are presented in Fig. 3,* and are a function only of a spatial group and the parameters of a lattice.

There is a definite interrelation between the growth and dissolution forms of crystals: the vertices of dissolution forms correspond to the faces of growth forms [16]. If (by analogy with Wulff) it is assumed that the faces of crystals dissolve at a rate inversely related to their reticular density, it becomes possible to introduce the concept of the ideal dissolution form of crystals [17].

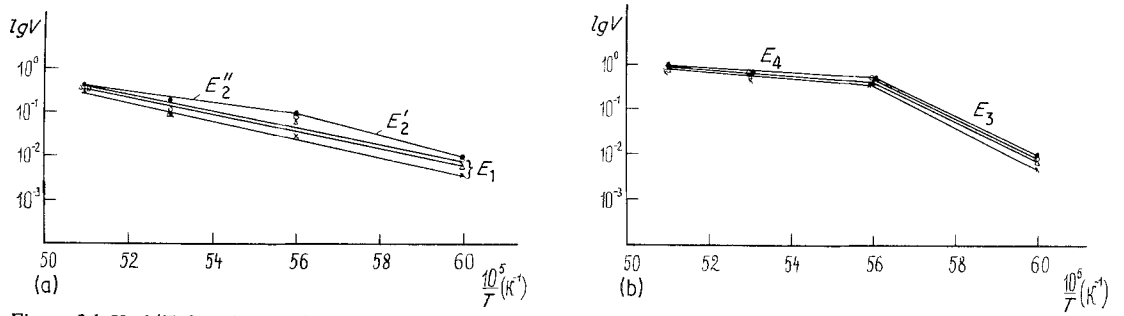

Figure 2 $lgV-1/T$ for thermochemical dissolution of spheres of (a) sapphire and (b) ruby along the crystallographic directions: × ⟨0 0 1⟩, △ ⟨1 1 0⟩, ○ ⟨0 2 1⟩, • ⟨1 1 3⟩.

*Each column shows the combined identical Wulff's ideal habits and each line shows the complete Wulff's ideal habits.

Here the ideal form of dissolution will be defined as a polyhedron whose vertices are the ends of vectors drawn from one point and perpendicular to the faces of Wulff's ideal habit; their lengths being equal to the corresponding interface distances.

Thus every ideal dissolution form corresponds to Wulff's ideal habit. All these forms are presented in Fig. 3. It must be said that the polyhedra with ideal dissolution forms may have curved faces, bent edges, blunt vertices (as is frequently observed during the dissolution of real crystals).

In some cases to determine the dissolution form of crystals, it is enough to know their Bravais group (Fig. 4).* In the corresponding square of Fig. 3 there is an ideal growth form and in Fig. 5 there is an ideal dissolution form. For example, the space group of CsI crystals is $Pm3m$ (the square KV in Fig. 4). The ideal growth form for CsI crystals is a cube (Fig. 3, CV), while the ideal dissolution form is an octahedron (Fig. 3, CI). Consequently the ideal growth form for these crystals is a cubo-octohedron (Fig. 3, CI), and the ideal dissolution form is a rhombododecahedron (Fig. 5, CI).

Dissolution of monocrystal spheres of CsI in the solution $CuCl_2 \cdot 2H_2O + C_2H_5OH$ [18, 19] and dissolution of monocrystal spheres of BaF_2 in HNO_3 (aqueous solution) [20] showed that their real forms correspond to the ideal forms. The real form of dissolution of CsI spheres are rounded octahedra. The real form of BaF_2 is rounded rhombododecahedra.

The bravais group of corundum is $R\bar{3}m$, $\alpha = 55°17'$ ($\alpha < 90°$) [1]. Corundum is presented in the square RI of Fig. 4. The ideal forms of growth and dissolution of corundum are the polyhedra in the squares RI in Figs 3 and 4, respectively. The ideal dissolution form of corundum is shown in Fig. 6a. It has the vertices :001:, :021: and :101:.

4.2. Comparison of the ideal and real dissolution forms of corundum

It is interesting to compare the ideal dissolution form of corundum with its real forms, obtained by different authors under different experimental conditions. The available data was reduced to a common system of indices by vertices (see the appendix) and for convenience of comparison these data are represented in Fig. 6b to e. The conditions of dissolution are given in the caption to Fig. 6.

In spite of different dissolution conditions the formation of a vertex :001: is observed in all cases and corresponds to the ideal dissolution form of corundum. The vertices with complicated

	I	II	III	IV	V
K	$Fm3m$	–	$Im3m$	–	$Pm3m$
Q	$I\frac{4}{m}mm$ $c/a>1$	$I\frac{4}{m}mm$ $c/a<1$	–	–	$P\frac{4}{m}mm$
R	$R\bar{3}m$ $\alpha<90°$	–	$R\bar{3}m$ $\alpha>90°$	–	–
O	$Immm$ Fmm	Fmm	Fmm	$Cmmm$	$Pmmm$
M	$C\frac{2}{m}$ $C\frac{2}{m}$	$C\frac{2}{m}$ $C\frac{2}{m}$	$C\frac{2}{m}$	$C\frac{2}{m}$	–
T	$P\bar{1}$	$P\bar{1}$	$P\bar{1}$	–	–
H	–	–	–	$P\frac{6}{m}mm$	–

Figure 3 The ideal growth forms of crystals.†

*If the Bravais groups are the same for the different habits (for example, the squares MI, MII, MIII), it is necessary to calculate the Delaunay reduction delta function [15].

†In each square of Fig. 3 the small polyhedron on the left is of the Bravais lattice type, on the right is the symbol of Delaunay's reduction. The matter is discussed in detail in [15].

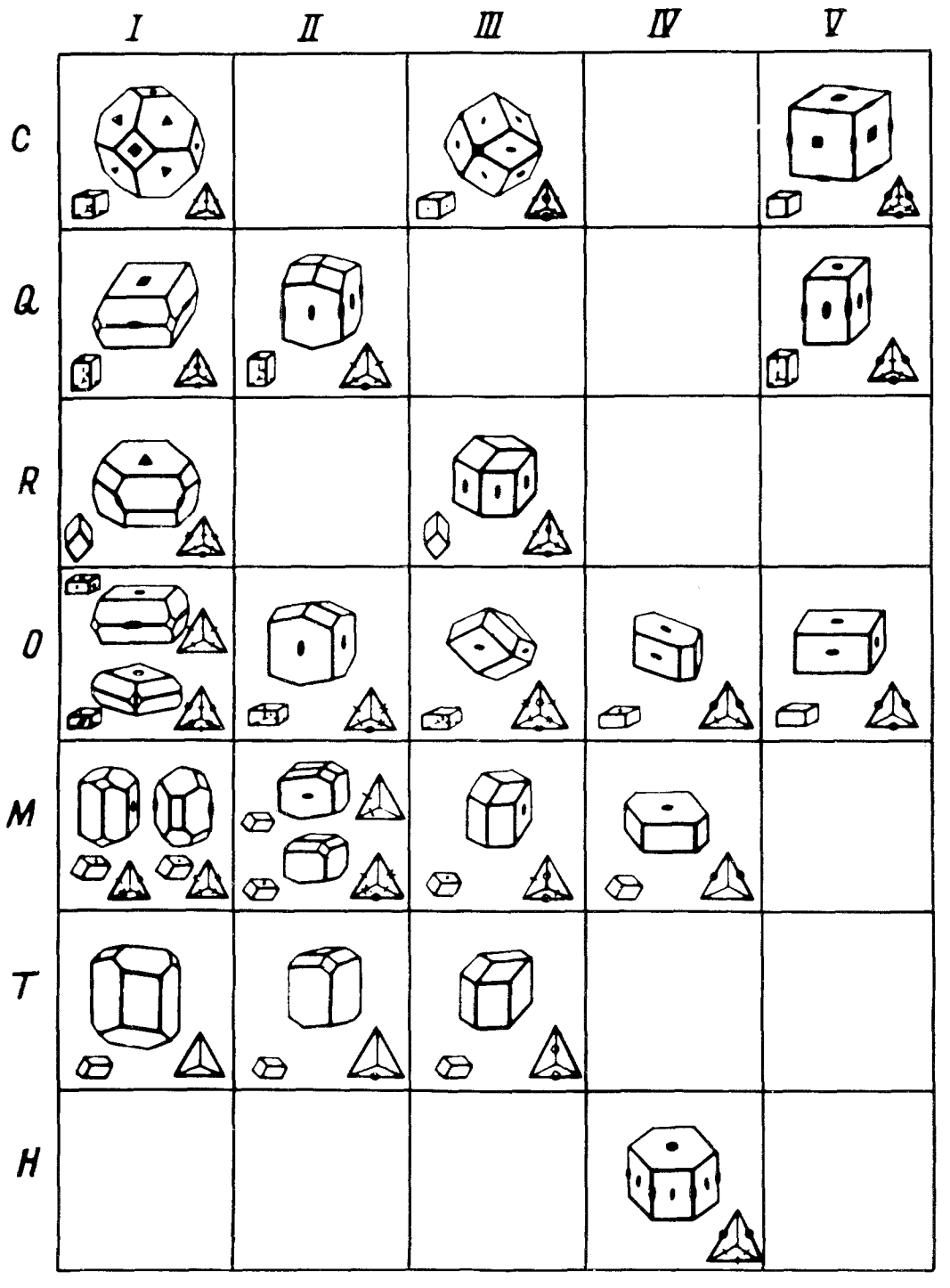

Figure 4 The distribution of Bravais groups in the table of ideal forms.

indexes (Fig. 6b and c) are absent in the ideal form (Fig. 6a). The change from dissolution of corundum in solutions and melts to dissolution in the gas phase leads to an increase in the number of vertices on the real forms (Fig. 6d and e). All vertices predicted by the ideal form appear on dissolution of ruby in CO. There also appears a series of additional vertices (:1 1 3: and :1 1 0:, Fig. 6a and e).

Earlier [11] the real dissolution form of the sapphire sphere was compared with forms of natural crystals and with the simple forms expected

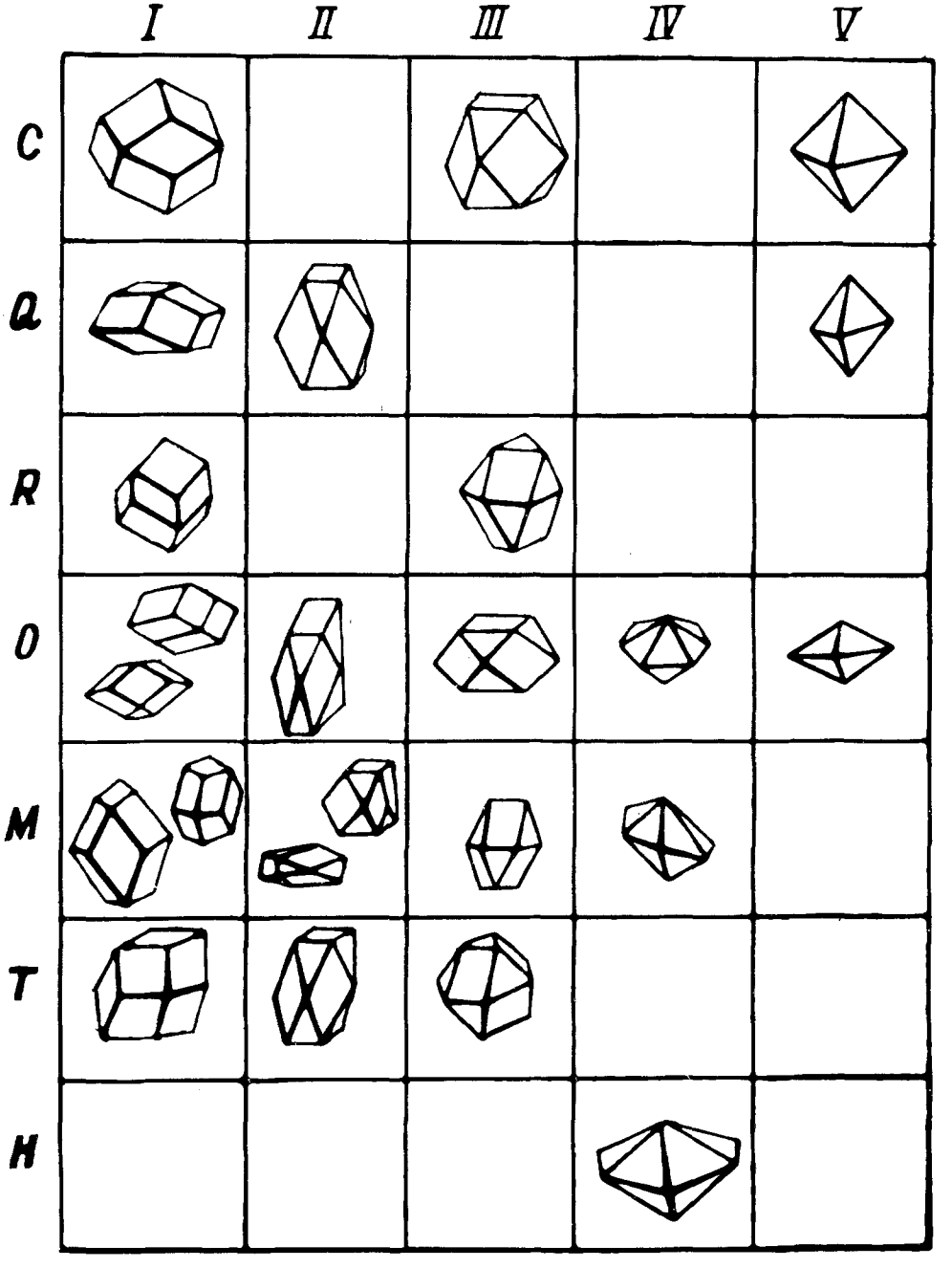

Figure 5 The ideal dissolution forms of crystals.*

on the basis of structure observations according to the Donnay–Harker [22] principle and Hartman's [23] data. If these data are compared with the ideal dissolution form, there is good correlation between the ideal growth form of corundum (and the ideal dissolution form) and the first three faces calculated by Hartman (the number of free bonds for the F-face in a cell). The data for the first three faces is presented in Table II. The three faces corresponding to the vertices on the ideal dissolution form of corundum have the largest interface distances [1]. It seems that the monocrystal sphere tends to form vertices on the surface, corresponding to the directions of the

*Each column shows combined identical ideal dissolution forms and each line shows the complete ideal dissolution forms.

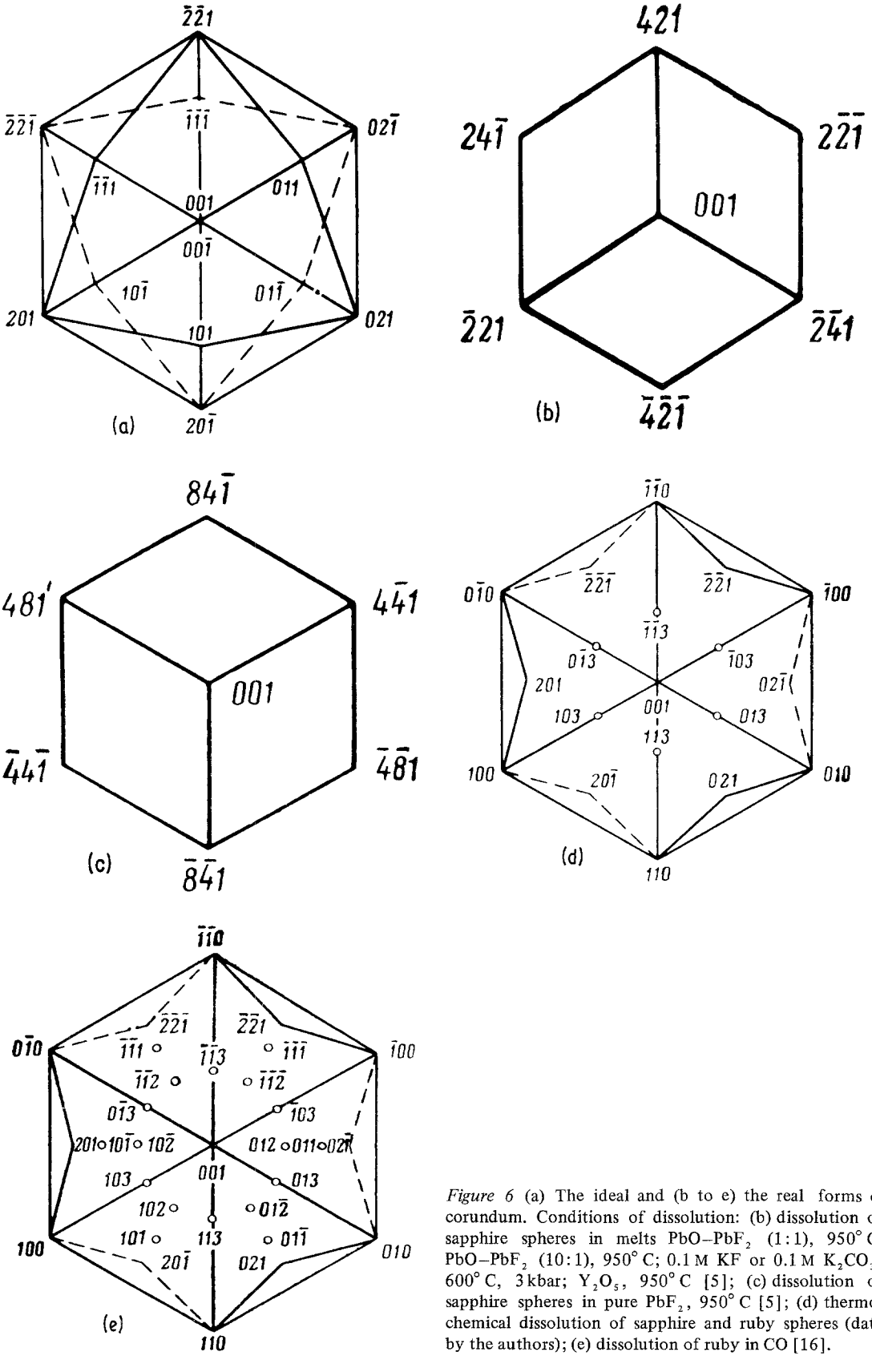

Figure 6 (a) The ideal and (b to e) the real forms of corundum. Conditions of dissolution: (b) dissolution of sapphire spheres in melts $PbO-PbF_2$ (1:1), 950° C; $PbO-PbF_2$ (10:1), 950° C; 0.1 M KF or 0.1 M K_2CO_3, 600° C, 3 kbar; Y_2O_5, 950° C [5]; (c) dissolution of sapphire spheres in pure PbF_2, 950° C [5]; (d) thermochemical dissolution of sapphire and ruby spheres (data by the authors); (e) dissolution of ruby in CO [16].

TABLE II Crystallographic forms of corundum

Vertices of the ideal forms	Faces of natural crystals in accordance with their frequency of observation	In accordance with the Donney–Harker principle	Number of free bonds for the F-Face in accordance with Hartman	
			In a cell	In a surface unit
0 0 1	0 0 1	1 0 1	1 0 1	1 0 1
0 2 1	1 0 1	0 1 2	1 1 0	0 0 1
1 0 1	2 2 3	1 1 0	0 1 2	0 2 1

maximum interface distances. The real experimental conditions, however, cause deviations in the sequence of vertex appearance in the order of decreasing interface distances.

4.3. Kinetics and chemistry of dissolution

Experiments on the dissolution of corundum spheres revealed an anisotropy of the dissolution rates and a difference in the dissolution rates of sapphire and ruby along corresponding crystallographic directions. The different dissolution rates of sapphire and ruby are due to their different structural defects, since an introduction of Cr^{3+} leads to formation of new centres of dissolution.

Our studies permit us to conclude that single corundum crystals will grow along the ⟨1 1 3⟩ direction at a maximum rate and along the ⟨0 0 1⟩ direction at a minimum rate [11].

Activation energies estimated from the dependence of $lgV-1/T$, permits suggestions to be made about the mechanism controlling the dissolution process. This mechanism may be connected with the diffusion process or with the rate of chemical reaction [24, 25]. In the former case the activation energy is relatively small (tenths of an eV), in the latter case this value is high (one or more eV). The activation energies for the thermochemical dissolution of corundum at temperatures of 1400 to 1700° C lie in the range 0.99 to 7.41 eV. This means that the process is controlled by the rate of chemical reaction. The bend in the $lgV-1/T$ curve at $T = 1500°$ C ($56 \times 10^5/T$ (K^{-1}) in Fig. 2) is connected with the additional participation of corundum sublimation. The experimental values of activation energies of dissolution of corundum 4.45 eV, 3.95 eV and 7.41 eV) were compared with the value of activation energy of sublimation of corundum at 1500° C (4 eV) [26]. The similarity between these values after the bend in Fig. 2 permits us to connect this bend with the sublimation of corundum.

When the {0 0 1} surface of sapphire was dissolved in hydrogen, $E = 2.47$ eV; thus, the chemical reaction rate controls this process, as in our case. When the {0 0 1} surface of sapphire was polished in H_3PO_4, $E = 0.07$ eV, and $9H_2SO_4$: H_3PO_4, $E = 0.1$ eV. Thus, the polishing in acids is limited by the diffusion of solvent to the surface of the crystal and by the diffusion of reaction products into the solution (Table III).

From Table III it may be concluded that

TABLE III Activation energy of dissolution of corundum

Crystal	Direction	Solvent	T (° C)	E (eV)	Source
Sapphire	1 1 3	CO	1400–1700	3.95	Data of the authors
	0 2 1		1400–1700	3.95	
	1 1 0		1400–1700	3.95	
	0 0 1		1400–1500	4.45	
			1500–1700	0.99	
Ruby	1 1 3	CO	1400–1500	7.41	
			1500–1700	1.48	
	0 2 1		1400–1500	7.41	
			1500–1700	1.48	
	1 1 0		1400–1500	7.41	
			1500–1700	1.48	
	0 0 1		1400–1500	7.41	
			1500–1700	1.48	
Sapphire	0 0 1	H_2	1200–1650	2.47	Calculation by the authors using the data from [7]
Sapphire	0 0 1	H_3PO_4	185–450	0.07	Calculation by the authors using data from [13]
	0 0 1	$9H_2SO_4$: H_3PO_4	250–300	0.10	

corundum dissolution in viscous mediums is controlled by diffusion, and in non-viscous (gas phase) by the rate of chemical reaction.

5. Conclusions

(1) By analogy with Wulff's ideal habits, ideal growth forms are considered the ideal dissolution forms of crystals. The ideal dissolution form of corundum is compared with its real forms obtained under different experimental conditions, and with simple forms, expected on the basis of structural considerations. It is shown that the ideal dissolution form of corundum corresponds to Hartman's habit.

(2) Anisotropy of the dissolution rates of sapphire and ruby spheres is revealed and the polar diagrams of dissolution rates are shown for the (0 0 1) face for the temperature range 1400 to 1700° C. It is shown that the (1 1 3) face has the highest dissolution rate. Ruby dissolves more readily than sapphire along all faces, however, (1 1 3) has a smoother surface in micro-relief.

(3) The activation energy values obtained from the $lgV-1/T$ curves show that the rate of chemical reaction between corundum and reagent controls the thermochemical dissolution of corundum. X-ray analysis shows that dissolution is accompanied by the formation of Al_4C_3.

Acknowledgements

The authors wish to express their thanks and appreciation to Dr R. V. Galiulin for his valuable advice and to B. M. Meerovich for his help in translating this paper into english.

Appendix On the relation between the co-ordinates of polyhedron vertices with Miller indices of its faces

Assuming that $x_1, y_1, z_1; x_2, y_2, z_2; x_3, y_3, z_3$ are three arbitrary points, let us use the following system of equations to find the Miller indices of a face containing these three points:

$$\begin{aligned} hx_1 + ky_1 + lz_1 &= 1; \\ hx_2 + ky_2 + lz_2 &= 1; \\ hx_3 + ky_3 + lz_3 &= 1. \end{aligned}$$

From which

$$h = \frac{\begin{pmatrix} 1y_1z_1 \\ 1y_2z_3 \\ 1y_3z_3 \end{pmatrix}}{\begin{pmatrix} x_1y_1z_1 \\ x_2y_2z_2 \\ x_3y_3z_3 \end{pmatrix}};$$

$$k = \frac{\begin{pmatrix} x_1 1z_1 \\ x_2 1z_2 \\ x_3 1z_3 \end{pmatrix}}{\begin{pmatrix} x_1y_1z_1 \\ x_2y_2z_2 \\ x_3y_3z_3 \end{pmatrix}};$$

$$l = \frac{\begin{pmatrix} x_1y_1 1 \\ x_2y_2 1 \\ x_3y_3 1 \end{pmatrix}}{\begin{pmatrix} x_1y_1z_1 \\ x_2y_2z_2 \\ x_3y_3z_3 \end{pmatrix}}. \qquad \text{(A1)}$$

Now let $h_1k_1l_1$, $h_2k_2l_2$, $h_3k_3l_3$ be the Miller indices of arbitrary faces. The point of intersection of these faces, as in the previous case, can be found by means of the following system of equations:

$$\begin{aligned} h_1x + k_1y + l_1z &= 1; \\ h_2x + k_2y + l_2z &= 1; \\ h_3x + k_3y + l_3z &= 1. \end{aligned}$$

Hence

$$x = \frac{\begin{pmatrix} 1k_1l_1 \\ 1k_2l_2 \\ 1k_3l_3 \end{pmatrix}}{\begin{pmatrix} h_1k_1l_1 \\ h_2k_2l_2 \\ h_3k_3l_3 \end{pmatrix}};$$

$$y = \frac{\begin{pmatrix} h_1 1l_1 \\ h_2 1l_2 \\ h_3 1l_3 \end{pmatrix}}{\begin{pmatrix} h_1k_1l_1 \\ h_2k_2l_2 \\ h_3k_3l_3 \end{pmatrix}};$$

$$z = \frac{\begin{pmatrix} h_1 k_1 1 \\ h_2 k_2 1 \\ h_3 k_3 1 \end{pmatrix}}{\begin{pmatrix} h_1 k_1 l_1 \\ h_2 k_2 l_2 \\ h_3 k_3 l_3 \end{pmatrix}} . \qquad \text{(A2)}$$

Equations A1 and A2 allow us to determine the relationship between the co-ordinates of polyhedron vertices and the Miller indices of its faces.

References

1. "Ruby and Sapphire" edited by L. M. Beljaev (Nauka Publishers, Moscow, 1974) (in Russian).
2. R. SCHEUPLEIN and P. GIBBS, *J. Amer. Ceram. Soc.* **43** (1960) 458.
3. W. J. ALFORD and D. J. STEPHENS, *ibid.* **46** (1963) 193.
4. J. A. CHAMPION and M. A. CLEMENCE, *J. Mater. Sci.* **2** (1967) 153.
5. B. SIESMAYER, R. HEIMAN, W. FRANKE and R. LACMANN, *J. Cryst. Growth* **28** (1975) 157.
6. H. M. MANASEVIT, *J. Electrochem. Soc.* **115** (1968) 434.
7. T. A. ZEVEKE, L. N. KORNEV and V. A. TOLOMASOV, *Kristallogr.* **13** (1968) 579.
8. V. S. PAPKOV, M. V. KLASSEN-NEKLUDOVA and V. G. GOVORKOV, Certificate of Authorship No. 182705, Bulletin of Inventions **12** (1966) 33.
9. V. G. GOVORKOV and A. E. SMIRNOV, Certificate of Authorship No. 548311, Bulletin of Inventions 8 (1977) 26.
10. V. N. VOIZEHOVSKII, *Kristallogr.* **13** (1968) 26.
11. H. S. BAGDASAROV, G. V. BEREZHKOVA, V. G. GOVORKOV and A. E. SMIRNOV, *J. Cryst. Growth* **22** (1974) 61.
12. V. G. GOVORKOV and A. E. SMIRNOV, *Kristallogr.* **24** (1979) 1095.
13. A. REISMAN, M. BERKENBLIT, J. CUOMO and S. A. CHAN, *J. Electrochem. Soc.* **118** (1971) 1653.
14. Yu. WULFF, "Selected Writings in Crystallophysics and Crystallography" (Technical and Theoretical Literature Publishing House, Moscow and Leningrad, 1952) (in russian).
15. B. N. DELAUNAY, R. V. GALIULIN and M. J. SHTOGRIN in "Selected Works" edited by O. Bravais (Nauka, Leningrad, 1974) p. 309 (in russian).
16. V. N. VOIZEHOVSKII and V. A. MOKIEVSKII, *Zap. Vsec. min. ob-va,* **93** (1964) 185.
17. A. E. SMIRNOV, R. V. GALIULIN and Yu. A. KHARITONOV, *Kristallogr.* **23** (1978) 434.
18. K. SANGWAL, A. A. URUSOVSKAYA and A. E. SMIRNOV, *Kristall. und Technik* **12** (1977) 149.
19. K. SANGWAL, A. A. URUSOVSKAYA and A. E. SMIRNOV, *Indian J. Pure Appl. Phys.* **16** (1978) 501.
20. A. E. SMIRNOV and A. A. URUSOVSKAYA, *J. Mater. Sci.* **15** (1980) 1183.
21. "Energies of Chemical Bonds", (Nauka Publishers, Moscow, 1974) (in russian).
22. Y. D. DONNEY and D. HARKER, *Amer. Mineral.* **13** (1937) 563.
23. P. HARTMAN, *Zap. Vses. Mineral.* **91** (1962) 672.
24. A. J. BRODSKII, "Physical Chemistry" Vol. 2 (Goshimizdat, Moscow-Leningrad) (in russian).
25. K. SANGWAL and S. K. ARORA, *J. Mater. Sci.* **13** (1978) 1977.
26. E. M. AKULONOK, V. V. PANTELEEV, E. A. FJODOROV and V. Y. HAIMOV-MALKOV, *Kristallogr.* **20** (1975) 873.

Received 8 May and accepted 17 October 1980.